

---

EFDA–JET–PR(04)20

S.E. Sharapov, R. Nazikian, B. Alper, D.N. Borba, E. De La Luna, J. Fessey,  
S. Hacquin, N.C. Hawkes, G.J. Kramer, S.D. Pinches, J. Rapp, D. Testa,  
N. Young and JET-EFDA Contributors

# Monitoring Alfvén Cascades with Interferometry on the JET Tokamak



# Monitoring Alfvén Cascades with Interferometry on the JET Tokamak

S.E. Sharapov<sup>1</sup>, R. Nazikian<sup>2</sup>, B. Alper<sup>1</sup>, D.N. Borba<sup>3</sup>, E. De La Luna<sup>4</sup>,  
J. Fessey<sup>1</sup>, S. Hacquin<sup>3</sup>, N.C. Hawkes<sup>1</sup>, G.J. Kramer<sup>2</sup>, S.D. Pinches<sup>5</sup>,  
J. Rapp<sup>6</sup>, D. Testa<sup>7</sup>, N. Young<sup>1</sup> and JET-EFDA Contributors\*

<sup>1</sup>EURATOM/UKAEA Fusion Association, Culham Science Centre, Abingdon, Oxon. OX14 3DB, UK

<sup>2</sup>Princeton Plasma Physics Laboratory, Princeton, NJ 08543-0451 USA

<sup>3</sup>Assoc. Euratom/IST, Centro de Fusão Nuclear, Av. Rovisco Pais, 1049-001 Lisboa, Portugal

<sup>4</sup>Assoc. Euratom-CIEMAT, Lab. Nacional de Fusion, Av. Complutense 22, Madrid, Spain

<sup>5</sup>Max-Planck Ins. Plasmaphys, Euratom Assoc., Boltzmannstraße 2, 85748 Garching, Germany

<sup>6</sup>Forschungszentrum Jülich GmbH, Euratom Association, 52425 Jülich, Germany

<sup>7</sup>CRPP/EPFL, Assoc. Euratom-Confederation Suisse, 1015 Lausanne, Switzerland

\* See annex of J. Pamela et al, "Overview of Recent JET Results and Future Perspectives",  
Fusion Energy 2002 (Proc. 19<sup>th</sup> IAEA Fus Energy Conf, Lyon 2002).

“This document is intended for publication in the open literature. It is made available on the understanding that it may not be further circulated and extracts or references may not be published prior to publication of the original when applicable, or without the consent of the Publications Officer, EFDA, Culham Science Centre, Abingdon, Oxon, OX14 3DB, UK.”

“Enquiries about Copyright and reproduction should be addressed to the Publications Officer, EFDA, Culham Science Centre, Abingdon, Oxon, OX14 3DB, UK.”

## ABSTRACT.

A microwave interferometry technique is applied for the first time for detecting a discrete spectrum of Alfvén Cascade (AC) eigenmodes excited with fast ions in reversed magnetic shear plasmas of the Joint European Torus (JET). The interferometry measurements of plasma density perturbations associated with ACs show an unprecedented frequency and time resolution of the eigenmodes superior to that obtained with external magnetic coils and with the electron-cyclotron emission radiometer. With the new technique, the spectrum of ACs is observed under a broader variety of conditions including plasmas with neutral beam injection, toroidally rotating plasmas and plasmas with toroidal current holes. The time-resolved measurements of ACs are used for monitoring the evolution of the safety factor and the density of rational magnetic surfaces in the region of maximum plasma current. The data obtained is used for developing reliable and reproducible scenarios with internal transport barriers on JET and provides an essential basis for assessing similar diagnostic technique in next-step fusion machines such as ITER.

## INTRODUCTION

Magnetohydrodynamic (MHD) spectroscopy that determines plasma characteristics via exciting and observing shear Alfvén Eigenmodes (AEs) at low power was proposed at the very beginning of magnetic nuclear fusion research [1]. During the past decade, the development of techniques for exciting Toroidal Alfvén Eigenmodes (TAEs) [2] with external antennas and with super-Alfvénic ions has increased the quality of information that MHD spectroscopy can deliver via the measurements of these AEs (see e.g. [3-7] and Refs. therein). More recently, a new class of frequency-sweeping discrete AEs was detected in JT-60U [8], JET [7], and TFTR [9] ‘advanced’ tokamak plasmas with reversed magnetic shear. These modes were called Alfvén Cascades (ACs) [7,10,11] and their applications for diagnosing the magnetic field topology in the ‘advanced’ tokamak have been assessed in [7,11-13].

The reversed-shear scenarios of tokamak operation work at a reduced inductive current and are investigated for achieving longer plasma discharges and ultimately reaching a steady-state tokamak operation at high fusion performance. These ‘advanced’ scenarios are focused on developing Internal Transport Barriers (ITBs), that determine regions in plasma where the plasma turbulence is suppressed and an improved insulation of thermal plasma is achieved (see e.g. [12, 13]). ITBs are best triggered by applying auxiliary plasma heating before the inductive current had fully penetrated into the plasma, so that the topology of equilibrium magnetic field  $\mathbf{B}$  is optimised by varying the safety factor

$$q(r) \equiv \mathbf{B} \cdot \nabla \zeta / \mathbf{B} \cdot \nabla \theta \quad (1)$$

which measures the ‘twist’ of the magnetic field lines  $\mathbf{B}$  as a function of the minor radius  $r$  of the torus. Here,  $r$  is constant on magnetic flux surfaces, and  $(\theta, \zeta)$  are appropriate poloidal and toroidal angle coordinates.

It was experimentally found on JET [12,13] that ITBs are triggered at a lower power of the auxiliary heating in plasmas with non-monotonic  $q(r)$ -profiles. It was also established, that the so-called ‘ITB triggering event’ observed as a sudden increase in the slope of electron temperature  $dT_e/dt$ , usually starts at magnetic surface  $r=r_{min}$  corresponding to a minimum  $q_{min}$  of  $q(r)$ -profile, at the time when  $q_{min}(t)$  passes an integer value [13]. A possible interpretation of the strong link between integer  $q$ - values and the spontaneous improvement of plasma confinement was given recently in terms of a reduced turbulent transport of the plasma due to the depleted density of rational magnetic flux surfaces around integer  $q$ - values [14,15].

Therefore, development of diagnostics, which can determine the time evolution of  $q_{min}(t)$ , is paramount for both reliable and reproducible scenarios with ITBs and for investigating the transport properties of the layer surrounding  $q_{min}$ , where the ITB starts from. MHD spectroscopy technique based on exciting the Alfvén Cascades and observing the AC frequency evolution in time is one of the possible options for diagnosing the temporal evolution of  $q_{min}(t)$ , since the AC eigenfrequencies are linked to the frequency of the Alfvén continuum at the point  $r=r_{min}$ , and the AC frequency  $\omega_{AC}$  traces the evolution of  $q_{min}(t)$  as [7, 10, 11]

$$\frac{d}{dt} \omega_{AC}(t) \approx \frac{d}{dt} \frac{V_A(r_{min})}{R_0} \left| n - \frac{m}{q_{min}(r,t)} \right| = m \frac{V_A}{R_0} \frac{d}{dt} q_{min}^{-1}(r,t). \quad (2)$$

Here,  $n, m$  are toroidal and poloidal mode numbers of a single AC mode,  $V_A(r) = |\mathbf{B}|/(4\pi\rho(r))^{1/2}$  is the Alfvén velocity and  $\rho(r)$  is the plasma mass density. In the past, such MHD spectroscopy was entirely reliant upon the AC measurements with external magnetic pick-up coils alone [7,11].

This Letter reports the first interferometry measurements of ACs driven with energetic ions accelerated by Ion Cyclotron Resonance Heating (ICRH) in plasmas of the JET tokamak. This interferometry technique, which detects plasma density perturbations associated with the ACs, shows an unprecedented frequency and time resolution of the eigenmodes, far superior to that obtained by external magnetic coils or by the Electron-Cyclotron Emission (ECE) radiometer reported earlier in [7,11]. The internal measurements of the density perturbation support the conclusions made for the TFTR DT experiments [9] that the techniques of measuring density perturbations associated with shear Alfvén waves can provide more detailed information on the modes than one can obtain with external magnetic coils alone.

In order to compare both the external and internal measurements of ACs on JET, a dedicated experiment was performed in low-density JET plasmas with Lower-Hybrid Current Drive (LHCD) and low power ICRH. This scenario is typical of the early phase of ‘advanced’ discharges when the inductive current is not fully penetrated into the plasma and  $q(r)$ -profile is decreasing in time on a resistive time scale. A system of O-mode reflectometers/interferometers, a multi-channel ECE radiometer, and external magnetic pick-up coils were set up for measuring perturbed density, perturbed electron temperature, and perturbed magnetic field respectively.

The O-mode reflectometer/interferometer on JET is located at the outer side of the torus (at

major radius  $R \approx 4\text{m}$ ) and it views the plasma horizontally through the magnetic axis with the line-of-sight perpendicular to the magnetic axis. The perturbed density signals associated with the ACs are obtained from the change of the phase of microwave beams reflecting from the inner wall of the torus (at major radius  $R \approx 2\text{m}$ ) in the interferometry regime and from the plasma in the O-mode reflectometry regime. The receiver measuring the returned microwave beam was connected to a digital converter with a sampling rate 1MHz and the data were recorded with 14 bit effective resolution for 3 s during discharges.

Figure 1(a) shows time traces of the input power and the plasma parameters from a  $B_T \approx 2.75\text{T}$ ,  $I_p \approx 1.7\text{MA}$  JET discharge, in which LHCD was applied during the current ramp-up phase in order to obtain a reversed-shear magnetic configuration. ICRH power was used for accelerating a small (few percent of the electron density) population of hydrogen minority ions to energies high enough for the ions to resonate with shear Alfvén waves. Figure 1(b) shows the fixed frequencies of the six-channel microwave beams used in the experiment versus the cut-off frequency determined by the plasma density. These beams operated in the interferometry regime if the central plasma density was below 0.43, 1.06, 1.44, 1.94, 2.54, or  $3.16 (\times 10^{19} \text{ m}^{-3})$  respectively for each of the beams above. Figure 2 shows both the interferometry and the external magnetic coil measurements of Alfvén modes excited by the fast ions in this discharge. The Alfvén frequency spectrum consists of many frequency-sweeping discrete modes observed in the frequency band from 40kHz to the TAE frequency range, 140kHz, in agreement with the well-established characteristics of the Alfvén Cascades [10,11] in shear-reversed tokamaks. Figure 2 (top) shows the interferometry measurements of the perturbed density associated with the modes, indicating that very high resolution in both time and frequency with high sensitivity can be achieved, so that ACs with toroidal mode numbers up to  $n = 16$  are observed. On the other hand, the magnetic probe data shown in Figure 2 (bottom) only detected ACs with mode numbers up to  $n = 5$  and during a much shorter time window. In addition, the magnetic signal was significantly polluted by irrelevant perturbed magnetic fields associated, for example, with ICRH beat waves.

In accordance with [7, 11], an Alfvén Cascade starts to be seen if the condition

$$m - nq_{min}(t) = 0 \quad (3)$$

becomes valid, where both  $m, n$  are integer values. It follows from (3), that for  $q_{min}(t)$  decreasing in time ACs of different mode numbers  $\mathbf{m}, \mathbf{n}$  are excited one-by-one, scanning the condition  $m/n = q_{min}(t)$  in time, so that Figure 2 (top) shows the sequence of possible rational values through which  $q_{min}(t)$  passes. Therefore, this Figure can be first used for monitoring the value of  $q_{min}(t)$  with a very high accuracy, up to  $\Delta q_{min} \approx 1/16$ , and, second, the appearance times of the ACs can be used as a diagnostics of rational magnetic surfaces passing through a layer at  $r \approx r_{min}$  associated with  $q_{min}(t)$ . In particular, Figure 2 (top) shows clearly that ACs of all possible mode numbers are excited simultaneously at  $t \approx 4.4$  sec and they form the so-called Alfvén grand-Cascade, which is

associated with  $q_{min}(t)$  passing an integer value [7, 11]. A clear gap in the density of ACs is observed just before the grand-Cascade showing the depletion of the rational  $m/n$  values as discussed in [14, 15].

A series of JET discharges similar to that shown in Figure 1 was performed with ICRH power scanned from its highest level of 5MW down to 1.4MW. High-quality data similar to that presented in Figure 2 (top) was obtained from the interferometer even at the lowest level of ICRH power. On the other hand, the external magnetic coils were only capable of detecting only a much smaller number of modes. Due to the lower level of ICRH power than in JET discharges described in [7, 11], the multi-channel ECE radiometer did not see any modes.

In order to investigate the interferometry-to-reflectometry transition and to estimate the value of the density perturbations due to ACs from the reflectometry, the plasma density was gradually increased by applying 2 MW of neutral beam injection (NBI) to a JET discharge with a scenario similar to that in Figure 1. Simultaneous measurement of the ACs and the  $q(r)$ -profile via the motional Stark effect (MSE) were performed. In the presence of the NBI, which fuels the plasma, the plasma density increased slowly from  $2.5 \times 10^{19} \text{ m}^{-3}$  to  $3.3 \times 10^{19} \text{ m}^{-3}$ , so that two higher-frequency channels of the O-mode reflectometer came into reflection at a certain time when an AC was observed. One reflectometry channel was reflecting from a layer close to the plasma centre at  $R \approx 3.13\text{m}$  while the other channel was reflecting from about half the minor radius of the plasma at  $R \approx 3.42\text{m}$ .

On both channels phase fluctuations were observed from the same Alfvén Cascade eigenmode with toroidal mode number  $n = 3$  and  $m = 6$  (determined from the set of magnetic coils). In order to estimate the density fluctuation level, the JET equilibrium was reconstructed with the MSE input for the weakly-reversed  $q(r)$  -profile, and the  $n = 3$  AC mode was computed for this equilibrium with the ideal MHD MISHKA [16] and NOVA-K [17] codes. Figure 3 shows the density fluctuations associated with the AC obtained from these codes. Due to the effect of ideal MHD compressibility in toroidal geometry [9, 17], the density perturbations associated with a poloidally symmetric magnetic perturbation of shear Alfvén mode have anti-ballooning character seen in Figure 3. This anti-ballooning structure of the density perturbations explains why the ACs are seen better with interferometry that reaches the inner side of the torus, while ballooning TAEs are better seen with external magnetic coils located at the outer side of the JET torus. The density fluctuation profile shown in Figure 3 was used as input for a 1D reflectometry code [18] in order to calculate the phase fluctuation due to the AC. The free parameter in this calculation, the density fluctuation level,  $\delta n/n_0$ , was adjusted to match the measured phase fluctuations. In this way a density fluctuation level of  $\delta n/n_0 \approx 0.3\%$  was obtained for the  $n = 3$  AC considered.

Further development of the interferometry technique followed after the series of dedicated experiments. By applying the interferometry technique routinely, it was noted that the ACs are best observed in the interferometry if the microwave beam frequency is just above (by 10-20%) the critical frequency determined by the central density of the plasma. In discharges with a growing density, a



multi-channel approach used on JET was therefore found to be very useful as the AC image is always seen on at least one interferometry channel. In such a way, the interferometry diagnostics of ACs allow to perform a permanent monitoring of the ACs, and to exploit it for  $q_{min}(t)$  diagnosis based on the clustering of ACs with different mode numbers in time along the lines described above [7, 11]. Most importantly, the monitoring of ACs provides reliable data for identifying exact timing of  $q_{min}(t) = integer$  events, which are most favourable for the ITB triggering, so that proper adjustments of the timing for the main auxiliary heating can be performed easily in order to develop reproducible and reliable ‘advanced’ scenarios with ITBs in JET.

In order to expand the interferometry technique to higher density JET discharges, an additional higher frequency channel was added to the high-frequency data acquisition system, in addition to the beams described above. The microwave beam of frequency 63.90 GHz allows the interferometry measurements in plasmas with densities as high as  $5.05 \times 10^{19} \text{ m}^{-3}$ , therefore expanding the range of the AC measurements to JET scenarios with high NBI power. Figure 4(a) shows time traces for a typical shear-reversed JET discharge with strong NBI heating while Figure 4(b) shows the microwave frequencies used in the experiments versus the cut-off profile. In this discharge, not only is the plasma density higher than in the discharge shown in Figure 1, but also the plasma rotates toroidally at high speed, driven by the unbalanced NBI, and the  $q(r)$ -profile has a current hole at the time of the AC observations. This data significantly differs from that shown in Figure 2(a). Although one can still recognize the Alfvén grand-Cascade at around  $t = 4.5\text{sec}$ , the modes now cover a much broader frequency band, up to 300kHz. The broader frequency range is caused by the Doppler shift  $\cong n\Omega_{rot}$  due to the strong toroidal plasma rotation, up to  $\Omega_{rot} \cong 2 \times 10^5 \text{ s}^{-1}$ , and the high mode numbers of the ACs, up to  $n = 10$ .

## SUMMARY

In summary, a new interferometry technique was developed for monitoring the discrete spectrum of Alfvén Cascade eigenmodes driven by ICRH-accelerated ions in fusion-grade ‘advanced’ JET tokamak plasmas with reversed magnetic shear. The interferometry measurements show an unprecedented frequency and time resolution of the eigenmodes and are used successfully for monitoring the evolution of the safety factor for developing scenarios with internal transport barriers. Similar technique based on higher frequency microwaves may be applied for diagnosing plasma of ITER-type tokamak-reactors with a shear-reversed equilibrium.

## ACKNOWLEDGEMENTS

This work was partly funded by Euratom and by the UK Engineering and Physical Sciences Research Council. This work was performed under the European Fusion Development Agreement.

## REFERENCES

- [1]. T. Stix, Phys. Fluids **1**, 308 (1958).
- [2]. C.Z. Cheng, L. Chen, and M.S. Chance, Ann.Phys. (N.Y.) **161**, 21 (1985).
- [3]. J. P. Goedbloed et al., Plasma Physics Controlled Fusion **35**, B277 (1993).
- [4]. H. A. Holties et al., Physics of Plasmas **4**, 709 (1997).
- [5]. G. Kramer, C.Z.Cheng, Y.Kusama, et al., Nuclear Fusion **41**, 1135 (2001).
- [6]. A. Fasoli et al., Plasma Physics Control. Fusion **44**, B159 (2002).
- [7]. S. E. Sharapov et al., Phys. Lett. A **289**, 127 (2001).
- [8]. H. Kimura, Y. Kusama, M. Saigusa, *et. al.* Nucl. Fusion **38**, 1303 (1998).
- [9]. R. Nazikian et al., Phys. Rev. Lett. **91**, 125003-1 (2003).
- [10]. H. L. Berk, D. N Borba, B. N. Breizman, *et. al.*, Phys. Rev. Lett. **87**, 185 (2002).
- [11]. S. E. Sharapov, B. Alper, H. L. Berk et al., Physics of Plasmas **9**, 2027 (2002).
- [12]. E. Joffrin et al., Plasma Physics Control. Fusion **44** (2002) 1739.
- [13]. E. Joffrin et al., Nuclear Fusion **43**, 1167 (2003).
- [14]. Y. Kishimoto et al, PPCF **41** A663 (1999).
- [15]. X. Garbet et al, Nucl. Fusion **43** (2003) 975
- [16]. A. B. Mikhailovskii et al., Plasma Phys. Rep. **23**, 844 (1997).
- [17]. C. Z. Cheng, Phys. Rep. **211**, 1 (1992).
- [18]. G. J. Kramer et al., Plasma Phys. Control Fus. **L10** (2002).

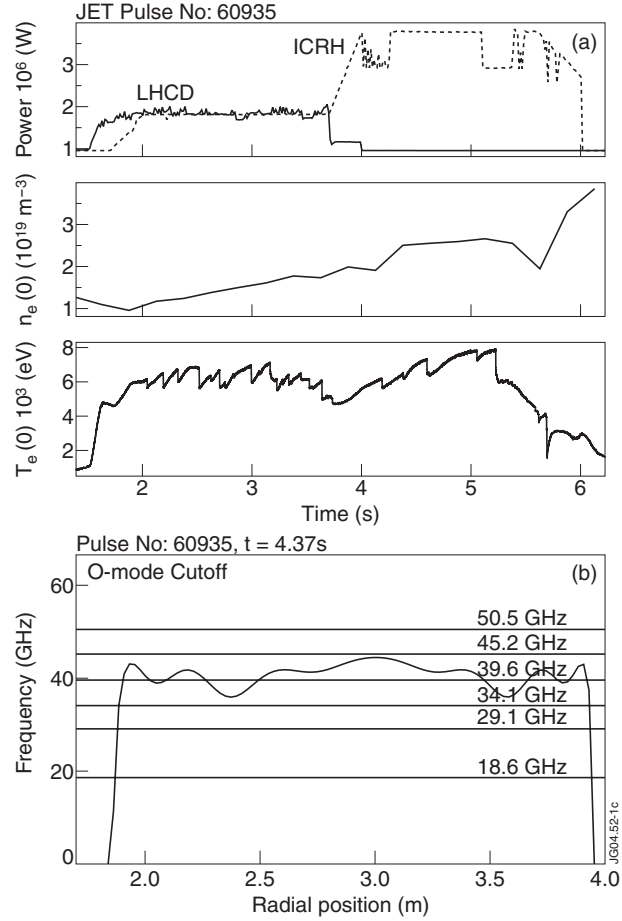


Figure 1. (a) Time traces of LHCD and ICRH power, on-axis electron density and central electron temperature in JET Pulse No: 60935. (b) Frequency of the O-mode cut-off as a function of major radius calculated from the measured electron density profile at  $t = 4.37\text{s}$ . Frequencies of the six microwave beams launched from  $R \approx 4\text{m}$  are also shown.

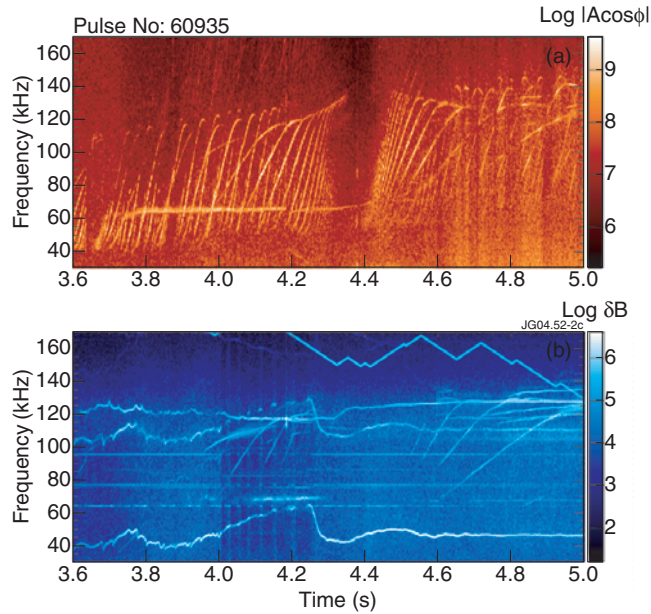


Figure 2. Fourier spectrograms of perturbations associated with shear-Alfvén eigenmodes obtained for the JET discharge shown in Figure 1. Top: interferometry measurements with microwave beam of 45.2GHz (critical density  $2.54 \times 10^{19} \text{ m}^{-3}$ ). Bottom: measurements with external magnetic pick-up coil. The observed frequency-sweeping discrete modes correspond to Alfvén Cascades with different toroidal and poloidal mode numbers.

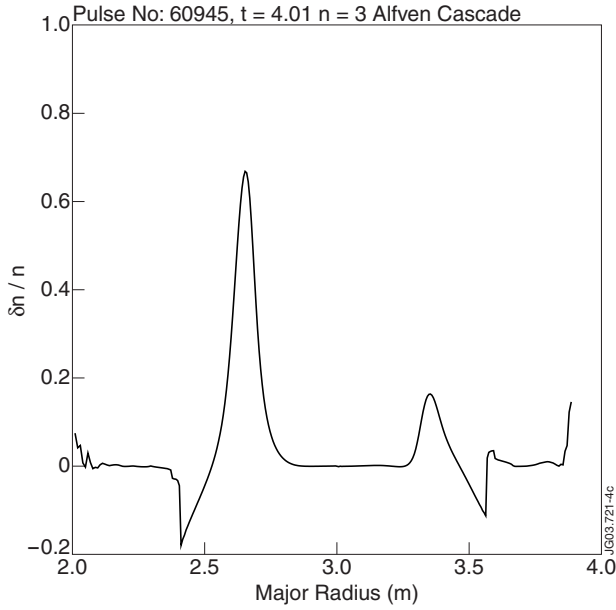


Figure 3. Profile of the density perturbations caused by the  $n = 3$ ,  $m = 6$ , Alfvén Cascade, as a function of major radius, computed with the NOVA-K code. The magnetic axis of the plasma is at  $R_0 \approx 3.0$  m.

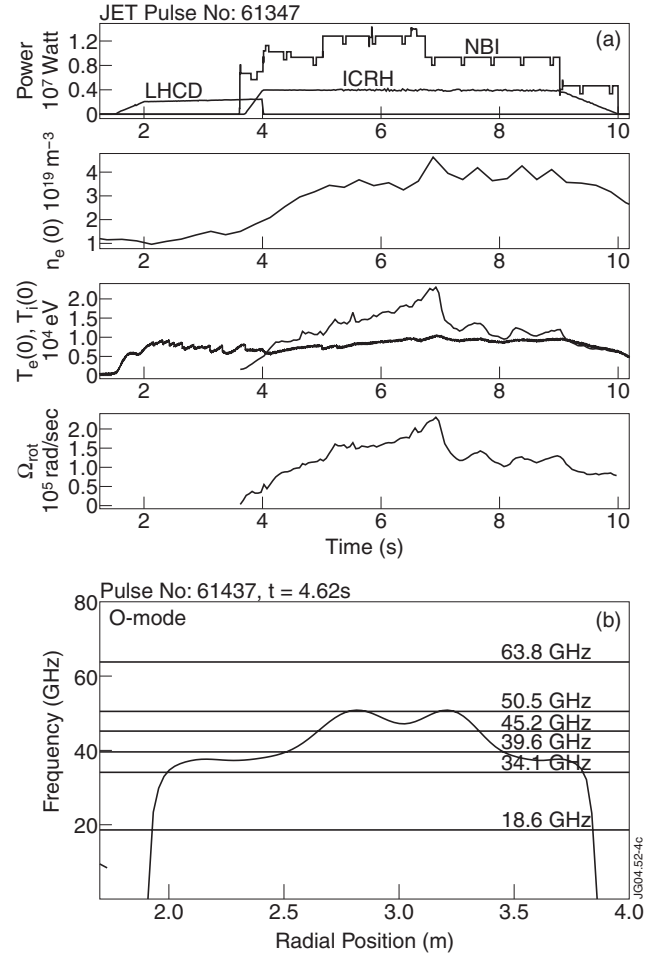


Figure 4. (a) Time traces of LHCD, ICRH and NBI power, on-axis plasma density, central electron and ion temperature, and toroidal plasma rotation in JET Pulse No: 61347. (b) Frequency of the O-mode cut-off as a function of major radius at  $t = 4.62$ s. Frequencies of the six microwave beams are shown.

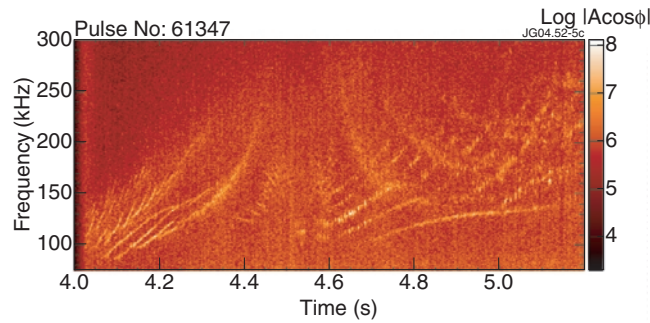


Figure 5: Interferometry measurement of Alfvén Cascades with microwave beam of 63.8GHz (critical density  $5 \times 10^{19} \text{ m}^{-3}$ ) in JET Pulse No: 61347 shown in Figure 4.